

Original Article

Spatiotemporal changes of tissue glycans depending on localization in cardiac aging

Yoko Itakura^a, Yasuko Hasegawa^b, Yurika Kikkawa^{a, c}, Yuina Murakami^{a, d},
Kosuke Sugiura^{a, c}, Chiaki Nagai-Okatani^e, Norihiko Sasaki^a, Mariko Umemura^d,
Yuji Takahashi^d, Tohru Kimura^c, Atsushi Kuno^e, Toshiyuki Ishiwata^b, Masashi Toyoda^{a, *}

^a Research Team for Geriatric Medicine (Vascular Medicine), Tokyo Metropolitan Institute of Gerontology, 35-2 Sakae-cho, Itabashi-ku, Tokyo 173-0015, Japan

^b Division of Aging and Carcinogenesis, Research Team for Geriatric Pathology, Tokyo Metropolitan Institute of Gerontology, 35-2 Sakae-cho, Itabashi-ku, Tokyo 173-0015, Japan

^c Laboratory of Stem Cell Biology, Department of Biosciences, Kitasato University School of Science, 1-15-1 Kitasato, Minami-ku, Sagami-hara, Kanagawa, 252-0373, Japan

^d Laboratory of Environmental Molecular Physiology, School of Life Sciences, Tokyo University of Pharmacy and Life Sciences, 1432-1 Horinouchi, Hachioji, Tokyo, 192-0392, Japan

^e Cellular and Molecular Biotechnology Research Institute, National Institutes of Advanced Industrial Science and Technology, 5 Central, Tsukuba, 1-1-1 Higashi, Tsukuba-city, Ibaraki 305-8565, Japan

ARTICLE INFO

Article history:

Received 5 August 2022

Received in revised form

30 November 2022

Accepted 22 December 2022

Keywords:

Cardiac tissue
Lectin microarray
Aging
Glycan profile
Microvessels

ABSTRACT

Introduction: Heart failure is caused by various factors, making the underlying pathogenic mechanisms difficult to identify. Since cardiovascular disease tends to worsen over time, early diagnosis is key for treatment. In addition, understanding the qualitative changes in the heart associated with aging, where information on the direct influences of aging on cardiovascular disease is limited, would also be useful for treatment and diagnosis. To fill these research gaps, the focus of our study was to detect the structural and functional molecular changes associated with the heart over time, with a focus on glycans, which reflect the type and state of cells. **Methods:** We investigated glycan localization in the cardiac tissue of normal mice and their alterations during aging, using evanescent-field fluorescence-assisted lectin microarray, a technique based on lectin-glycan interaction, and lectin staining. **Results:** The glycan profiles in the left ventricle showed differences between the luminal side (medial) and wall side (lateral) regions. The medial region was characterized by the presence of sialic acid residues. Moreover, age-related changes in glycan profiles were observed at a younger age in the medial region. The difference in the age-related decrease in the level of α -galactose stained with *Griffonia simplicifolia* lectin-IB4 in different regions of the left ventricle suggests spatiotemporal changes in the number of microvessels. **Conclusions:** The glycan profile, which retains diverse glycan structures, is supported by many cell populations, and maintains cardiac function. With further research, glycan localization and changes have the potential to be developed as a marker of the signs of heart failure.

© 2022, The Japanese Society for Regenerative Medicine. Production and hosting by Elsevier B.V. This is an open access article under the CC BY-NC-ND license (<http://creativecommons.org/licenses/by-nc-nd/4.0/>).

Abbreviations: ACG, *Agrocybe cylindracea* galectin; α -SMA, alpha smooth muscle actin; BPL, *Bauhinia purpurea alba* lectin; Calsepa, *Calystegia sepium* agglutinin; ConA, *Canavalia ensiformis* lectin; DAPI, 4',6-diamidino-2-phenylindole; DBA, *Dolichos biflorus* agglutinin; ECA, *Erythrina cristagalli* agglutinin; ECM, extracellular matrices; EMT, endothelial-to-mesenchymal transition; FITC, fluorescein isothiocyanate; Gal, galactose; GalNAc, N-acetylgalactosamine; GlcNAc, N-acetylglucosamine; GSL-I, *Griffonia simplicifolia* lectin I; HE, hematoxylin-eosin; LEL, *Lycopersicon esculentum* lectin; LTL, *Lotus tetragonolobus* lectin; MAH, *Maackia amurensis* hemagglutinin; MAL-I, *Maackia amurensis* lectin I; Man, mannose; NPA, *Narcissus pseudonarcissus* agglutinin; PBS, phosphate-buffered saline; PCA, principal component analysis; PHA-L, *Phaseolus vulgaris* leucoagglutinin; PNA, *Arachis hypogaea* agglutinin; RCA120, *Ricinus communis* agglutinin I; SBA, *Glycine max* agglutinin; SNA, *Sambucus nigra* agglutinin; SSA, *Sambucus sieboldiana* agglutinin; STL, *Solanum tuberosum* lectin; TJA-I, *Trichosanthes japonica* agglutinin I; UDA, *Urtica dioica*; VVA, *Vicia villosa* agglutinin; WFA, *Wisteria floribunda* agglutinin; WGA, *Triticum vulgaris* agglutinin (wheat germ agglutinin).

* Corresponding author.

E-mail address: mtoyoda@tmig.or.jp (M. Toyoda).

Peer review under responsibility of the Japanese Society for Regenerative Medicine.

<https://doi.org/10.1016/j.reth.2022.12.009>

2352-3204/© 2022, The Japanese Society for Regenerative Medicine. Production and hosting by Elsevier B.V. This is an open access article under the CC BY-NC-ND license (<http://creativecommons.org/licenses/by-nc-nd/4.0/>).

1. Introduction

Age is a major risk factor for cardiovascular diseases, including heart failure, whose prevalence has been increasing with an aging society [1]. Further, heart failure can be caused by various factors, making the underlying pathogenic mechanisms difficult to identify. To promote a more positive patient outcome, early diagnosis of cardiovascular diseases is the key for treatment. However, it can be challenging for the elderly to detect the signs of cardiac dysfunction and seek medical attention, and they often overlook physiological symptoms; thus, heart failure tends to gradually worsen over time.

Some age-related diseases, such as aortic valve stenosis and atrial fibrillation, can increase the risk of developing cardiovascular diseases [2–5]. Further, acute myocardial infarction and angina pectoris caused by narrowing or thrombus in major vessels, such as the coronary artery, induce various complications, including left ventricular free wall rupture, ventricular septal perforation, and papillary muscle rupture [6–8].

More recently, it has been reported that elderly patients with coronavirus disease 2019 (COVID-19) can have aggravated symptoms accompanied with related cardiovascular complications [9–11]. SARS-CoV-2, the virus that causes COVID-19, can cause vascular inflammation through the angiotensin-converting enzyme 2 receptor, a glycoprotein on the cell surface, and can thus destroy cardiovascular integrity, particularly in elderly patients with advanced arteriosclerosis [12–16].

The specific functions of cardiac tissue are supported by numerous cell populations which change with aging [17]. Recently, it has been reported that various diseases are induced by senescent cells [18–20], and that senescent cells are related to cardiovascular aging and age-related cardiovascular diseases [21]. Understanding tissue alterations that occur with aging could be useful for early disease diagnosis as well as the development of effective therapies against age-related heart failure. However, suitable biomarkers for distinguishing healthy aging from impaired organ function associated with heart failure are lacking. Therefore, it is important to elucidate the mechanisms underlying cardiovascular diseases, including the structural and functional changes in cell populations with aging, in order to develop optimal therapies.

Glycans are suitable candidates for a spatiotemporal analysis of molecular changes; these molecules are located on cell surfaces, and their profiles can differ based on cellular characteristics or functional changes [22]. We previously showed that the amount of sialic acid residues on cell surface proteins decreases during cellular senescence and human aging [23]. Moreover, Miura et al. [24] reported that the amount of high-branched *N*-glycans on plasma proteins in supercentenarians is higher than that in younger individuals.

The lectin microarray is an analytical approach that can be used to obtain the global glycan profiles of both *N*- and *O*-glycans in glycoprotein samples [25–27]. Matsuda et al. [28] successfully used lectin microarrays to analyze pathomorphological features of glycans on glycoproteins extracted from small tissue sections and reported that the technique has high sensitivity. This technique has also been used to show differences of glycan structures in cancerous and non-cancerous areas [29]. Further, a combination of laser microdissection and lectin microarray was used to perform glycome mapping (glycan profiling of the whole body) in mouse models [30].

An analysis tool, LM-GlycomeAtlas, has been developed to allow user access to glycome data that can be obtained from the laser microdissection-assisted lectin microarray [31]. The combination of glycan data from these analysis tools and animal tissues will be useful in understanding changes in the glycan level and localization

in different organs. However, the spatiotemporal changes remain unclear. To overcome this, it is important to capture normal age-related changes and then use these to identify disease-specific changes. Therefore, we aimed to investigate glycan levels and localization in serial sections of the hearts of female mice using a lectin microarray technique to monitor molecular changes during aging. We chose to profile glycan changes during aging using female mice because the prevalence of cardiac diseases in post-menopausal females is significantly high. Furthermore, we then determined the cardiac tissue condition of aged mice, which is the reference standard for not developing the disease.

2. Materials and methods

2.1. Tissue section preparation

All animal experiments were approved by the Animal Ethics and Experimentation Committee of the Tokyo Metropolitan Institute of Gerontology (TMIG) (No. 17020), and all methods were performed at TMIG in accordance with the relevant guidelines and regulations. C57BL/6N female mice, aged 2 months ($n = 4$), 6 months ($n = 3$), 12–14 months ($n = 4$), and 23–25 months ($n = 4$), were purchased from Japan SLC, Inc., (Shizuoka, Japan) and reared in the TMIG animal facility for aging. All animals were anesthetized with 50 mg/kg pentobarbital sodium salt through intraperitoneal injection and sacrificed through continuous perfusion with saline followed by 4% paraformaldehyde solution in phosphate-buffered saline (PBS) into the heart. Isolated perfused hearts were immediately re-fixed in 4% paraformaldehyde. The fixed hearts were embedded in paraffin and cut, horizontally, into 3–5 μm serial sections for immunohistochemistry and 5 μm serial sections for lectin microarray analysis (Fig. 1).

2.2. Lectin microarray analysis

Three generations of female mice, three each aged 2 months, 12–14 months, and 23–25 months, were used for lectin microarray analysis (Fig. 1a and Supplementary Table S1). The hematoxylin-stained paraffin-embedded thin sections were mounted on a polyethylene naphthalate membrane slide. Two serial tissue sections were cut to 0.5 mm^2 in the same region using LMD7000 (Leica Microsystems, Wetzlar, Germany) and collected into microtubes. Proteins from the dissected tissue fragments were extracted as previously described [30]. Briefly, 200 μL of 10 mM citrate buffer (pH 6.0) was added to each tissue fragment and incubated at 95 °C for 1 h. A 50% slurry of 20 μm cellulose (Sigma–Aldrich, Co., St. Louis, MO, USA) was added to the tube and then washed twice with PBS. After centrifuging at 20,000 $\times g$ for 1 min at 4 °C, the slurry was solubilized with 20 μL of PBS containing 0.5% Nonidet P-40 (Nacalai Tesque, Inc., Kyoto, Japan) and subjected to three cycles of sonication (15 s each). Thereafter, the sonicated solution was incubated on ice for 1 h and collected by centrifugation at 20,000 $\times g$ for 1 min at 4 °C. The supernatant was resuspended in 20 μL PBS and labeled with 10 μg of Cy3 mono-reactive dye (GE Healthcare, Buckinghamshire, UK) at 25 °C for 1 h in the dark. The volume of the reaction solution was adjusted to 100 μL with probing buffer (Tris-buffered saline containing 1% Triton X-100, 1 mM CaCl_2 , and 1 mM MnCl_2 ; pH 7.4) and incubated at 25 °C for 2 h. The Cy3-labeled solution (60 μL) was applied to a LecChip (GlycoTechnica, Yokohama, Japan) and incubated at 25 °C for approximately 17 h. Thereafter, the LecChip was washed three times with probing buffer and then analyzed on an evanescent-field fluorescence scanner (GlycoStation™ Reader 1200, GlycoTechnica) using the GlycoStation™ Tools Signal Capture 1.0 and GlycoStation™ Tools

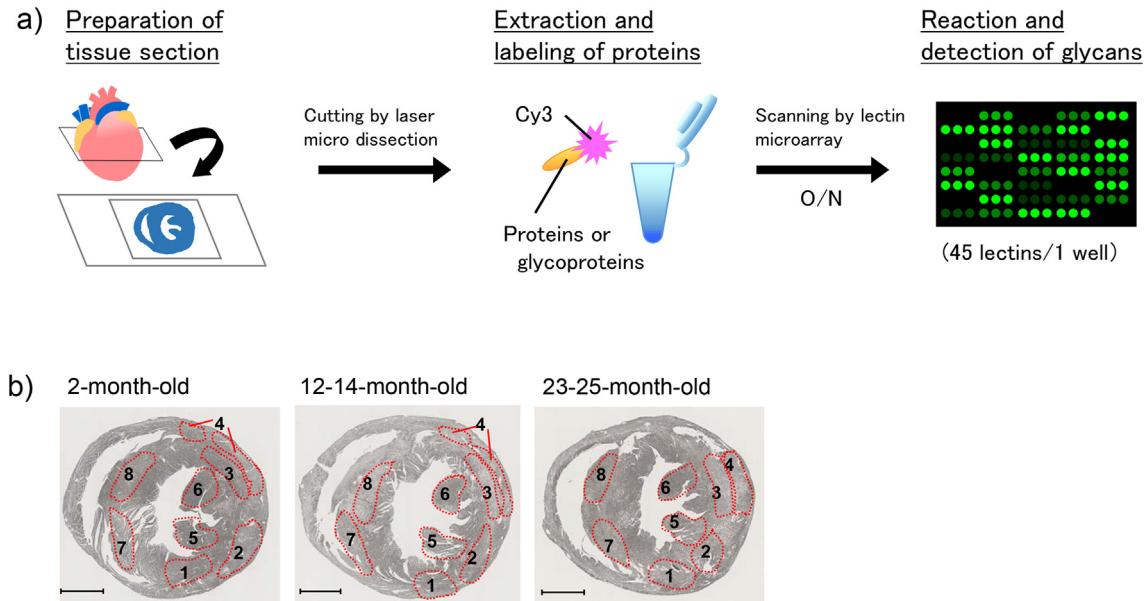


Fig. 1. Lectin microarray analysis of glycoproteins in mouse cardiac tissue (a) Schematic illustration of lectin microarray analysis of tissue glycoproteins. The hearts of female mice were cut at or near the midportion of the cardiac ventricle. Collected sections were incubated in 10 mM citrate buffer (pH 6.0) and sonicated with phosphate-buffered saline (PBS), containing 0.5% Nonidet P-40, and then glycoproteins were extracted. (b) The short-axes of the female mouse cardiac tissues in the three age groups (2, 12–14, 23–25 months; $n = 3, 3, 3$, respectively) and each region of analyzed glycoproteins (No. 1 and 2, ventral left ventricular wall; No. 3 and 4, dorsal left ventricular wall; No. 5 and 6, papillary muscle; and No. 7 and 8, ventricular septum).

Pro 1.0 software applications. Scanning data were selected under appropriate gain conditions, which satisfied fewer than 63,000 net intensities of all signals, and averaged data were analyzed for glycan characterization. For accurate comparative analysis, the data were used with average-normalization [32].

2.3. Immunohistochemistry, lectin staining, and quantitative analysis

To validate the morphology, all deparaffinized and activated 3 μm tissue sections were stained with hematoxylin-eosin (HE). Tissue staining was performed according to the manufacturer's instructions. Five micrometer-thick deparaffinized sections were stained with *Triticum vulgaris* agglutinin (wheat germ agglutinin; WGA), *Erythrina cristagalli* agglutinin (ECA), *Maackia amurensis* lectin I (MAL-I), or a combination of *Griffonia simplicifolia* lectin I (GSL-I) B4 and anti- α -smooth muscle actin (α -SMA) antibody for phenotypic analysis. Briefly, the deparaffinized slices were activated using an autoclave with Histofine Deparaffinizing Antigen Activation Solution (pH 6.0) (#415281; Nichirei Biosciences Inc., Tokyo, Japan) at 120 °C for 20 min. The tissue sections were washed with PBS, incubated at 25 °C for 10 min in Biotin Blocking System (# \times 059030-2; Agilent Technologies, Inc., Santa Clara, CA, USA) (setting of 0.1% avidin solution and 0.01% biotin solution), and thereafter washed with PBS for 5 min. The sections were incubated with Carbo-Free Blocking Solution (#SP-5040-125; Vector Laboratories Inc., Burlingame, CA, USA) containing 0.1% Tween 20 for 1 h. The slides were then washed with PBS, and thereafter, the tissue slices were incubated with the anti- α -SMA antibody (#ab5694, 1:200; Abcam plc, Cambridge, UK) in PBS or fluorescein isothiocyanate (FITC)-conjugated WGA (#L4895; 1:300; Sigma-Aldrich Co.) in Carbo-Free Blocking Solution at 25 °C for 1 h or 10 $\mu\text{g}/\text{mL}$ for each of the following: FITC-conjugated ECA (#FL-1141; Vector Laboratories Inc.), or FITC-conjugated MAL-I (#FL-1311; Vector Laboratories Inc.) at 4 °C overnight in PBS. Following a wash step with PBS, the sections were incubated with 10 $\mu\text{g}/\text{mL}$ of Dylight594-conjugated GSL-IB4 (#DL-1207; Vector Laboratories

Inc.) in combination with anti- α -SMA antibody at 4 °C overnight in PBS. The tissue sections were then washed with PBS and incubated at 25 °C for 1 h in a PBS solution containing anti-Rabbit IgG-AF488 (1:1000; Thermo Fisher Scientific) and anti- α -SMA antibodies. After washing with PBS, the cells were stained with 4',6-diamidino-2-phenylindole (DAPI) for 10 min and then mounted with the Fluorescent Mounting Medium (Agilent Technologies Inc.). The stained sections were evaluated using a NanoZoomer (Hamamatsu Photonics, Shizuoka, Japan) for HE staining and Fluoview (Olympus Digital Solutions Co., Tokyo, Japan), DB6B (Leica Microsystems), and BZ-X710 (Keyence Co., Osaka, Japan) for WGA, ECA, and MAL-I, and a combination of α -SMA and GSL-IB4 staining, and then the hybrid cell count was determined using the BZ-X710 software (Keyence Co.) for WGA enclosing and a ratio of GSL-IB4 per tissue area. Signal intensities of ECA and MAL-I staining were calculated with pixels using ImageJ 1.53. Detection of microvessels was performed in the area without α -SMA staining.

2.4. Enzymatic treatment for the lectin microarray

After Cy3-labeling, 20 μL of the reaction solution was digested into sialic acid with sialidase A (#GK80040; Agilent Technologies Inc.) or α 2-3sialidase (#4455; Takara Bio Inc., Shiga, Japan), according to the manufacturer's instructions. The volume of the solution was adjusted to 100 μL with probing buffer and incubated at 4 °C until use. For analysis, 60 μL of the solution was applied to the lectin microarray. The data obtained for mice aged 2 and 23–25 months were compared with those without enzymatic reactions and the difference was calculated using the following formula: difference = \log_2 (signal intensity with sialidase/signal intensity without sialidase).

2.5. Statistical analysis

Lectin microarray data were analyzed using hierarchical clustering and principal component analysis (PCA) by means of pair-wise comparison, using ANOVA (<http://lgsun.grc.nia.nih.gov/ANOVA/>)

(false discovery rate <0.05). The mean value of the lectin microarray data was used for each PCA. The data are presented as the mean \pm standard error of the mean or median with quartiles. Significant differences in nucleus staining and WGA and GSL-IB4 data were evaluated using the Kruskal–Wallis test ($p < 0.05$), and those in ECA or MAL data were evaluated using an unpaired t test, using IBM SPSS Statistics 26 (Stats Guild Inc., Japan).

3. Results

3.1. Glycan structure reflects changes in cell morphology

To determine the morphological changes in the mice hearts due to aging, the cellular morphology of two regions (papillary muscle and left ventricular wall) was examined. The thin sections of both regions were stained with HE and WGA, a lectin known to stain the cellular membrane [33]. When comparing the mice hearts at the age of 2 months, 12–14 months, and 23–25 months using HE staining, the number of nuclei per area significantly decreased with increasing age, while the nucleus size remained the same in both regions (Fig. 2a). These morphological changes were also observed in other cardiac areas (Supplementary Fig. S1a; ventricular spectrum). These results suggest that cells, especially those in the cytoplasm, acquire hypertrophy with age.

In the sections stained with WGA, cellular size at 23–25 months in the papillary muscle region appeared to be enlarged; the cellular edge was obscure, and adhesion between adjacent cells was not tight, unlike in 2-month-old mice (Fig. 2b left). These changes were similar in other areas of the heart (Fig. 2b right, left ventricular wall; Supplementary Fig. S1b, ventricular spectrum). The position where WGA staining was performed at 23–25 months in both regions was interrupted and widening was observed (Fig. 2b; arrows and arrowheads, respectively). Although there was no clear significant difference in cell enlargement, the results of this staining suggest possible molecular changes in the plasma membrane or pericellular region.

3.2. Glycan mapping of mouse cardiac tissues

To investigate the characteristics of glycans in mouse cardiac tissues, eight parts of the short-axis slices from normal female mouse hearts, including the left ventricular wall (No. 1 and 2, ventral sides; 3 and 4, dorsal sides), the papillary muscle (No. 5 and 6), and the ventricular septum (No. 7 and 8), were analyzed for three age groups (2 months, 12–14 months, and 23–25 months) using the lectin microarray (Fig. 1b). A broad variety of lectin signals were detected at each location for all ages with *Calystegia sepium* agglutinin (Calsepa), *Agrocybe cylindracea* galectin (ACG), *Solanum tuberosum* lectin (STL), *Lycopersicon esculentum* lectin (LEL), and *Canavalia ensiformis* lectin (ConA) showing the highest signal intensities (Supplementary Fig. S2 and Supplementary Table S2).

Further, the glycan profiles of the eight areas of the hearts of 2-month-old mice were analyzed in detail using PCA. All points of papillary muscle (No. 6) and ventricular septum (No. 8) were placed in regions II and III, which were defined by sialic acid-binding lectins (*Sambucus nigra* agglutinin, SNA; *Sambucus sieboldiana* agglutinin, SSA; *Trichosanthes japonica* agglutinin I, TJA-I; ACG, and MAL-I), chitin-binding lectins (*Urtica dioica*, UDA; LEL, STL, and WGA) that also bind to sialic acid residues in a multivalent manner [34], and mannose-binding lectins (ConA and *Narcissus pseudonarcissus* agglutinin, NPA) (Fig. 3a and Table 1). These indicate that both areas were characterized by sialic acid residues. One other ventricular septum (No. 7) part and a papillary muscle (No. 5) part were positioned near the center of PC1.

Furthermore, the ventral left ventricular wall (No. 1 and 2) was mainly located in regions I and IV, which were defined by O-glycan-binding lectins such as *Wisteria floribunda* agglutinin (WFA), *Glycine max* agglutinin (SBA), *Vicia villosa* agglutinin (VVA), *Dolichos biflorus* agglutinin (DBA), *Arachis hypogaea* agglutinin (PNA), *Bauhinia purpurea alba* lectin (BPL), GSL-IA4, and GSL-IB4. These regions were also characterized by large-branched and asialo N-glycan-binding lectins, such as *Phaseolus vulgaris* leucoagglutinin (PHA-L) and ECA, respectively. On the other hand, the dorsal left ventricular wall (No. 3 and 4) was located farther from the center of PC1 in regions I and IV. These results suggest that glycan clusters extracted from cardiac tissues could be roughly distinguished in each region. In a cross section of the heart, the orientation of the myocardial layers could be seen. Based on the shape of the myocardial layer, the wall side of the left ventricle was designated as the “lateral” and the luminal side of the heart as the “medial” region.

To determine whether these region-specific glycan characteristics continue temporally, we examined glycan profiles in two left ventricular wall regions (No. 1, 2 and No. 3, 4) and the medial region (No. 5–8) among the mice aged 2, 12–14, and 23–25 months. The glycan profiles of each group of the ventral sides (No. 1 and 2) and the dorsal sides (No. 3 and 4) of the left ventricular wall, and the medial area of the left ventricle (No. 5–8) in the three age groups, were distinctly clustered on PC1 (Fig. 3b). Further, all medial areas (No. 5–8) among the three age groups were characterized by sialic acid-related lectins (SNA, SSA, TJA-I, ACG, STL, UDA, and LEL). Further, data for groups of the ventral sides (No. 1 and 2) and the dorsal sides (No. 3 and 4) of the left ventricular wall and the medial side (No. 5–8) at each age were analyzed by hierarchical clustering. The glycan profiles between the left ventricular wall and the medial area were clearly differentiated. Additionally, the left ventricular wall was further distinctly differentiated into the ventral and dorsal sides (Fig. 3c). These hierarchical clustering data also indicated the degree of variation in glycan profiles as “distance”. In both left ventricular walls, there was a high degree of similarity in the profiles at 2 and 12–14 months. The same was observed in the profiles for the medial side at 12–14 and 23–25 months. This suggests that the ventral and dorsal sides of the left ventricular wall had similar glycan characteristics, which continued temporally, and that glycan clusters extracted from cardiac tissues could be roughly distinguished between the “lateral” (No. 1–4) and “medial” (No. 5–8) regions of the left ventricle.

To confirm the above observation, we examined glycan profiles in the left ventricular wall region (No. 1–4) and medial region (No. 5–8) among the mice in the three age groups (2, 12–14, and 23–25 months). The glycan profiles of each group of the left ventricular wall (No. 1–4) and medial area of the left ventricle (No. 5–8) in the three age groups were clearly differentiated into regions II/III and I/IV, which were characterized by several specific lectins (Fig. 3d). The glycan profiles between the left ventricular wall and medial area in the hierarchical clustering were also clearly differentiated, similar to the results in the PCA (Fig. 3e). The profiles at 2 and 12–14 months in the left ventricular wall were clustered together, while in the medial side, those at 12–14 and 23–25 months formed close clusters. These results indicate that the changes in glycan profiles occurred at an earlier stage in the medial side than in the left ventricular wall. They also show that the change in glycan profiles on the medial side was greater than that in the left ventricular wall.

3.3. Sialic acids are well characterized in papillary muscles

High levels of sialic acid were maintained temporally in the medial region of the heart (No. 5–8). We investigated whether

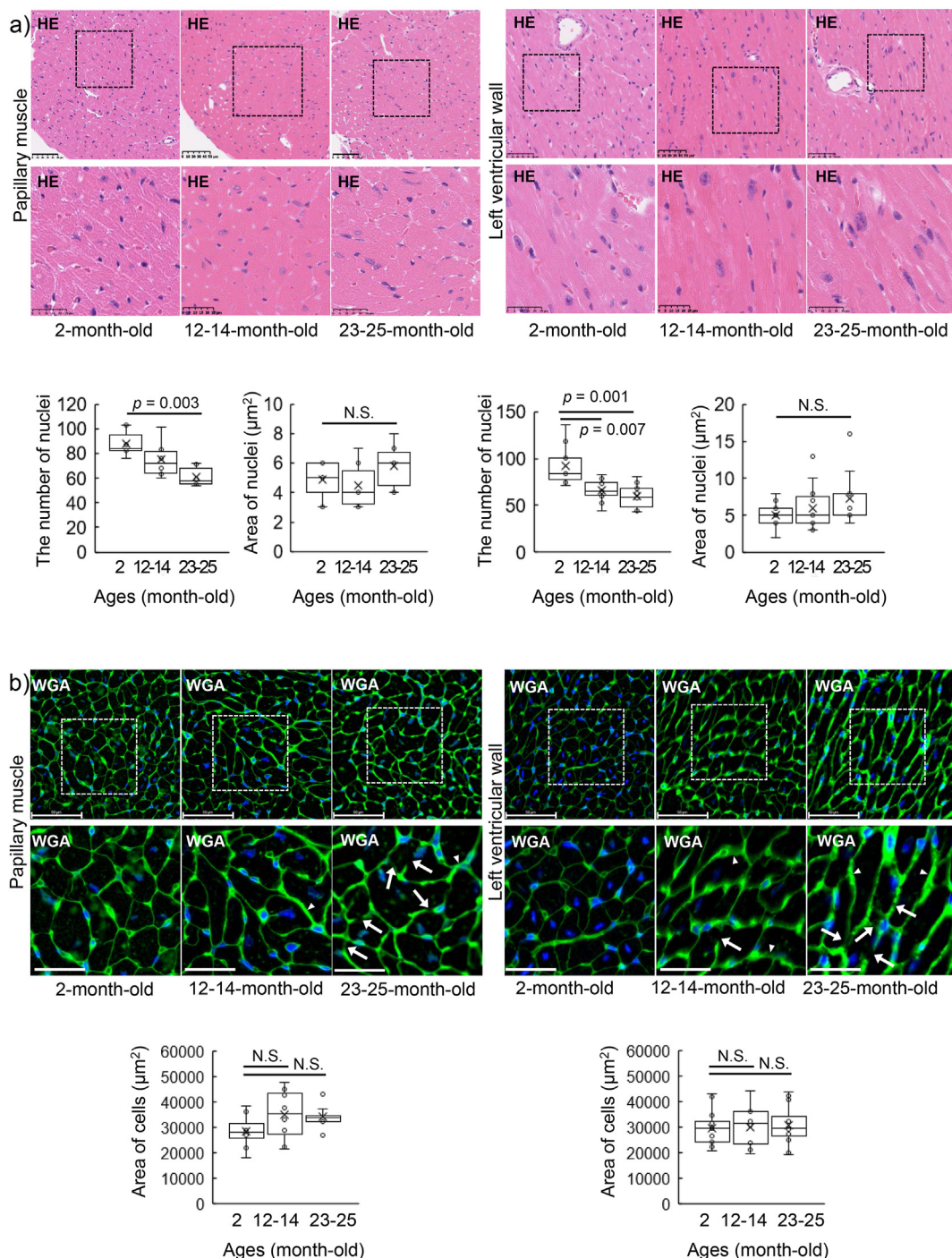


Fig. 2. Cardiac morphology in aging. (a) The short-axes of cardiac tissues from female mice aged 2, 12–14, and 23–25 months were stained with hematoxylin-eosin (HE) in the papillary muscle and the left ventricular wall regions on a set of the left and right sides ($n = 3$ per group). Lower panels show the magnified view of the squared area in the upper panels. Scale bars are 50 and 25 μm for the upper and lower panels, respectively. The number and area of nuclei in each region are shown on the left and right graphs, respectively ($n = 6–7$ per group). (b) The short-axes of cardiac tissues of female mice aged 2, 12–14, and 23–25 months were stained with wheat germ agglutinin (WGA) (green) and 4',6-diamidino-2-phenylindole (DAPI) (blue) in the papillary muscle and the left ventricular wall regions on a set of the left and right sides ($n = 8–13$ locations; 3–4 mice per group). Lower panels represent the magnified view of the squared area in the upper panels. Scale bars are 50 and 25 μm for the upper and lower panels, respectively. Size of cell per unit area in each region enclosed with WGA in three aged mice was calculated. $P < 0.05$. N.S. = no significant difference. Arrow shows areas where lines are interrupted. Arrowhead shows areas where the cell spacing is widening.

specific sialic acid structures were present and if there were changes between 2-month-old and 23–25-month-old mice, based on the changes in lectin signals with sialidase treatment in the papillary muscle. To evaluate the presence of sialic acid residues, we analyzed using some sialic acid- and asialo-binding lectins. In

the samples treated with sialidase A, which digests the α 2-3 and 2–6 linkages of sialic acid, the signal intensities of sialic acid-recognizing lectins (*M. amurensis* hemagglutinin, MAH; SNA, SSA, TJA-I, MAL-I, ACG, and WGA) were drastically decreased in 2-month-old mice (the reduction ranging from 30% to 90%). On the

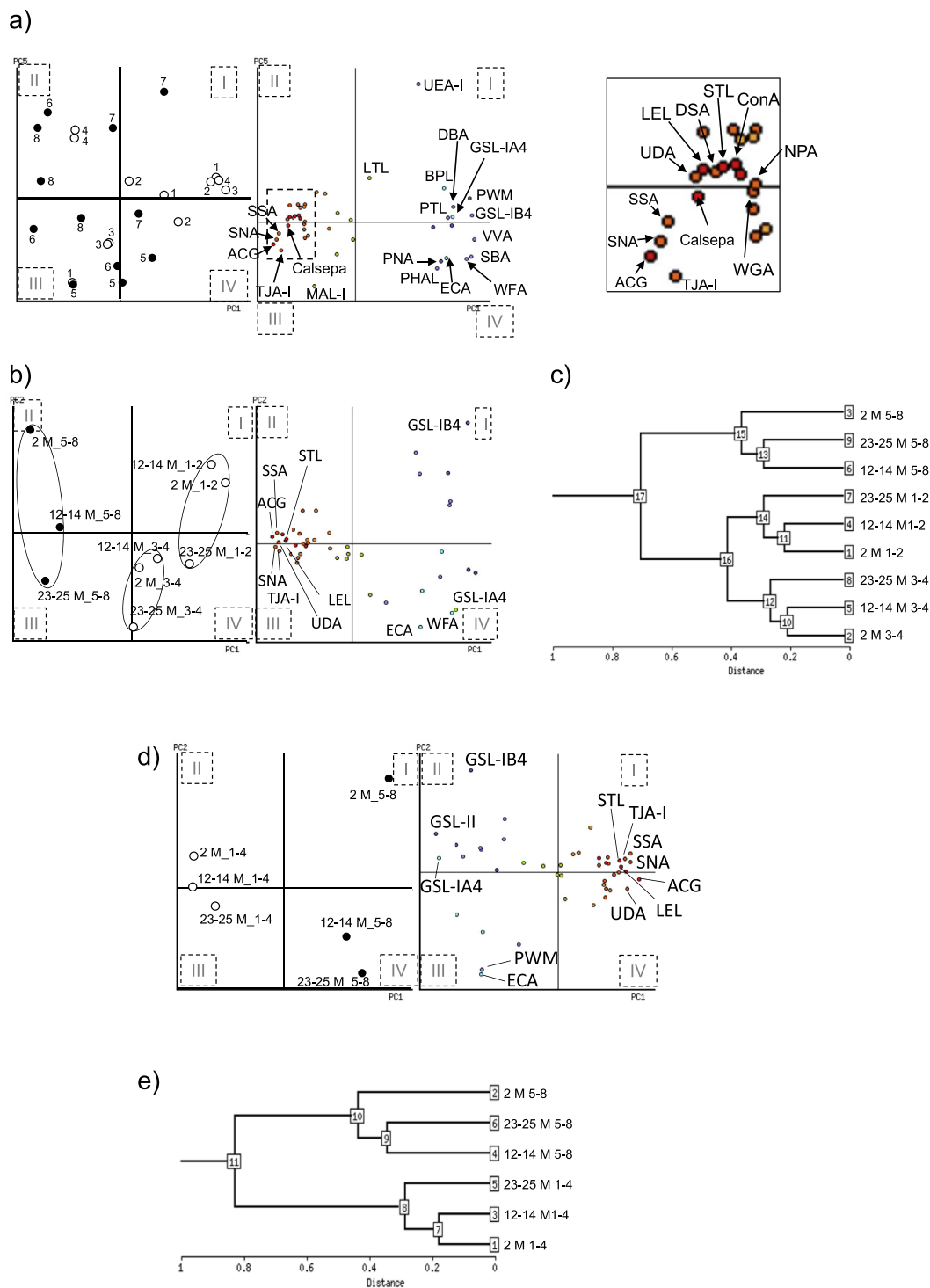


Fig. 3. Statistical analysis of lectin microarray data (a) Eight regions of three 2-month-old female mice were individually assessed using principal component analysis (PCA). Open and closed circles represent areas No. 1–4 and 5–8, respectively. Left panel in the bi-plot: Cardiac areas; right panel in the bi-plot: Lectin replications. The right panel shows a magnified view of the squared area in the left panel. (b) The average of three mice per group for the ventral sides (No. 1 and 2) and the dorsal sides (No. 3 and 4) of left ventricular wall, and medial side (No. 5–8) in 2-, 12–14-, and 23–25-month-old mice were performed. Open and closed circles represent areas No. 1–4 and 5–8, respectively. Left panel in the bi-plot: Cardiac areas; right panel in the bi-plot: Lectin replications. (c) The average of three mice per group for the three areas in left ventricles in 2-, 12–14-, and 23–25-month-old mice were determined by hierarchical clustering. The nodes are numbered in the order of sample input and in order of proximity to the branching point of the hierarchy. (d) The average of three mice per group for the lateral and medial left ventricle in 2-, 12–14-, and 23–25-month-old mice were analyzed using PCA. Open and closed circles represent areas No. 1–4 and 5–8, respectively. Left panel in the bi-plot: Cardiac areas; right panel in the bi-plot: Lectin replications. (e) The average of the lateral and medial left ventricles in three mice per group of mice aged 2, 12–14, and 23–25 months was determined by hierarchical clustering. The nodes are numbered in the order of sample input and in order of proximity to the branching point of the hierarchy.

Table 1
Glycan signatures in cardiac tissue areas.

Tissue areas	Left ventricular wall (No. 1–4)	Medial area of left ventricle (No. 5–8)
Glycans	Gal α GalNAc α GalNAc β 1-4GlcNAc Gal β 1-4GlcNAc	α 2-6sialic acid α 2-3sialic acid [GlcNAc] n Man

Gal, galactose; GalNAc, N-acetylgalactosamine; GlcNAc, N-acetylglucosamine; Man, mannose.

Table 2
Relative intensities relating to sialic acid- and galactose-binding lectins in the papillary muscle.

Lectins	Sialidase A (+)				α 2-3sialidase (+)											
	2 (m/o) ^a .		Ave.		23–25 (m/o)		Ave.		2 (m/o)		Ave.		23–25 (m/o)		Ave.	
MAL-I	0.2	0.2	0.2	0.2	0.3	0.2	0.1	0.2	0.4	0.1	0.2	0.2	0.3	0.2	0.2	0.2
SNA	0.1	0.1	0.1	0.1	0.1	0.0	0.1	0.1	–	–	–	–	–	–	–	–
SSA	0.1	0.2	0.2	0.2	0.2	0.2	0.2	0.2	–	–	–	–	–	–	–	–
TJA-I	0.1	0.2	0.2	0.2	0.4	0.4	0.4	0.4	–	–	–	–	–	–	–	–
ACG	0.4	1.2	0.4	0.7	0.9	1.1	0.8	0.9	0.5	0.5	0.4	0.5	1.5	0.9	1.1	1.1
MAH	0.3	0.3	0.4	0.3	0.3	0.3	0.3	0.3	0.5	0.3	0.5	0.4	0.5	0.6	0.4	0.5
WGA	0.8	0.5	0.6	0.6	1.0	1.0	0.9	1.0	0.8	0.6	0.7	0.7	0.7	0.6	0.5	0.6
LTL	–	–	–	–	–	–	–	–	3.5	3.6	2.9	3.4	1.3	1.4	1.4	1.4
ECA	7.2	9.0	8.6	8.3	1.8	2.0	1.6	1.8	16.3	7.0	9.9	11.0	4.6	4.0	2.1	3.6
RCA120	0.6	6.8	5.5	4.3	1.0	1.3	1.0	1.1	2.3	2.7	2.9	2.7	1.2	1.5	1.1	1.2
WFA	7.2	3.9	10.2	7.1	0.7	1.3	1.1	1.0	8.5	4.1	8.1	6.9	9.4	4.5	3.2	5.7

The data were averaged after a comparison with those of the no-sialidase sample ($n = 3$). Ave., average.

^a The m/o shows month old.

other hand, the signal intensities of lectins (*Ricinus communis* agglutinin I, RCA120; ECA, and WFA) that recognize glycan residues appearing when sialic acids were removed were increased (Supplementary Fig. S3a, and Table 2). In contrast, in the 23–25-month-old mice, the signal intensities of ACG, WGA, RCA120, and WFA showed little change (Supplementary Fig. S3a, and Table 2). The signal intensity of ECA was increased 1.8-fold, but the change was very small compared to 2-month-old mice. The difference between 2 and 23–25 months of age was the most pronounced in galactose- or N-acetylgalactosamine-binding lectins (Fig. 4a). These results suggest that some types of sialic acid residues were removed from the glycoproteins in the papillary muscles and that the diversity of these residues was decreased with aging.

To further validate the binding of sialic acid, the samples extracted from thin sections were incubated with α 2-3sialidase. In the 2-month-old mice, the signal intensities of MAL-I, ACG, MAH, and WGA were decreased, whereas the signal intensities of ECA, RCA120, WFA, and *Lotus tetragonolobus* lectin (LTL) (no binding to α 2-3-linked sialylated structure, such as sialyl-Le^x) were increased (Supplementary Fig. S3b and Table 2). On the contrary, in the 23–25-month-old mice, the changes in the signal intensities of ACG, LTL, ECA, and RCA120 due to enzyme treatment were minor (Supplementary Fig. S3b and Table 2), while the changes in the signal intensities of WGA and WFA were almost the same as those at 2 months of age. The difference between 2 and 23–25 months of age was the most pronounced in galactose- or N-acetylgalactosamine-binding lectins, similar to the results with sialidase A (Fig. 4b).

These results indicate that the residues of both α 2-6 and 2-3-linked sialic acid and a sialyl-Le^x glycan structure were contained in the papillary muscle and that the amounts of their sialic acid residues, at least α 2-3-linked sialic acid residues, in 23–25-month-old mice were less than those in 2-month-old mice. Moreover, these results suggest that the diversity of sialic acid on proteins was reduced with aging.

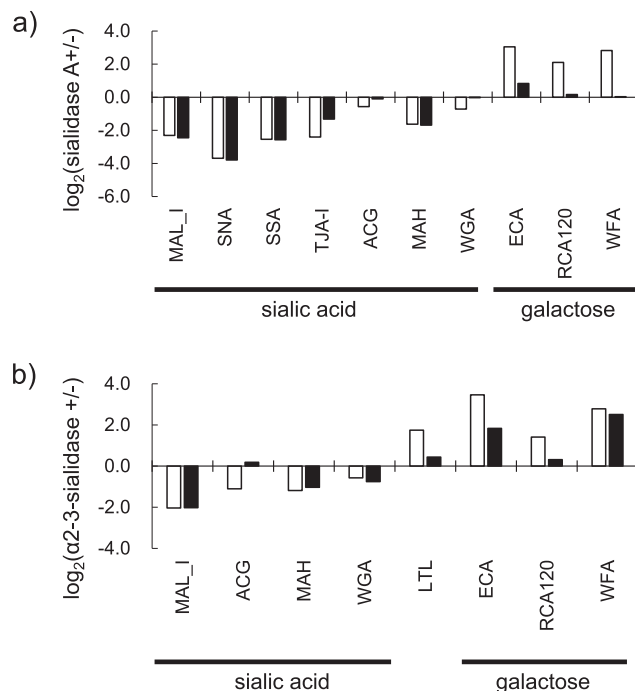


Fig. 4. The age-related changes observed in sialylated glycans of the medial region (a) Relative intensities relating to sialic acid-, galactose-, and N-acetylgalactosamine-binding lectins in the papillary muscle with sialidase A treatment are shown. The average relative intensity of three mice in 2-month-old and 23–25-month-old groups (open and closed bars, respectively) was analyzed individually with or without sialidase treatment ($n = 3$ per group). Bar graph represents the difference between signal intensity with and without sialidase treatment as \log_2 value. (b) Relative intensities of sialic acid-, galactose-, and N-acetylgalactosamine-binding lectins in the papillary muscles with α 2-3-sialidase treatment are shown. The average relative intensity of three mice in the two age groups was analyzed individually with or without sialidase treatment ($n = 3$ per group). Bar graph represents the difference between signal intensity with and without sialidase treatment as \log_2 value.

3.4. The change in glycan characteristics in cardiac tissue with aging

To further investigate the age-related changes in glycan profiles in the vicinity of the left ventricle, we focused on the eight areas and examined the glycan profiles in the three age groups. In most areas, the profiles changed with aging from regions III/IV to I/II (Fig. 5a). In particular, the glycan profiles of the medial side, such as No. 5, 6, and 8, severely changed with aging. Nevertheless, the changes with aging in the profiles of sialic acid-related lectins, which characterized the medial area, were minor. On the other hand, ECA was shown to be a characteristic lectin in aged mice, while GSL-IB4 was associated with young mice. These results suggest that several glycan types throughout the cardiac tissue changed with aging, although the rate of change varied from area to area.

To validate the age-related glycan changes with lectin microarray data, the tissue sections from 2-month-old and 23–25-month-old mice were stained with ECA and MAL-I. The signal intensity of ECA in 23–25-month-old mice was stronger and more distinct than that in 2-month-old mice, in both the papillary muscle and left ventricular wall regions (Fig. 5b and d; upper panel). Although the increase in mean value of ECA staining in papillary muscle was very slight, intercellular staining was particularly prominent in the left ventricular wall at 23–25 months of age. On the other hand, the signal intensity of MAL-I in both regions in

23–25-month-old mice was lower than that in 2-month-old mice (Fig. 5c and d; lower panel). The tissue staining results indicate that the amount of exposed galactose residue, as part of lactosamine, on multi-antennary *N*-glycans increased with aging. These results suggest that age-related changes in glycan profiles occurred throughout the tissue, with some glycan structures changed markedly in certain regions.

3.5. Changes in glycan levels in microvessels with aging

The lectin microarray data also showed that the signal intensity of GSL-IB4 was specific in 2-month-old mice, and that the rate of change in glycan profiles was different between the medial and lateral sides of the left ventricular wall (Figs. 5a and 3e). GSL-IB4 is known to bind to an endothelial cell marker, and the anti- α -SMA antibody is used as a marker for smooth muscles, indicating arteries and veins. To examine tissue changes involving glycans, the sections were stained with GSL-IB4 and the anti- α -SMA antibody (Supplementary Fig. S4). The area stained with GSL-IB4 in the cardiac tissue was denoted as microvessels, and the microvessel density around the cardiomyocytes was evaluated. The tissue sections of the mice in the different age groups (2, 6, 12–14, and 23–25 months) were compared, for both the medial and lateral areas of the left ventricular wall. The area of the papillary muscle stained with GSL-IB4 alone was shown to decrease between 2 and 6 months of age. The intensity of the stained area of the papillary

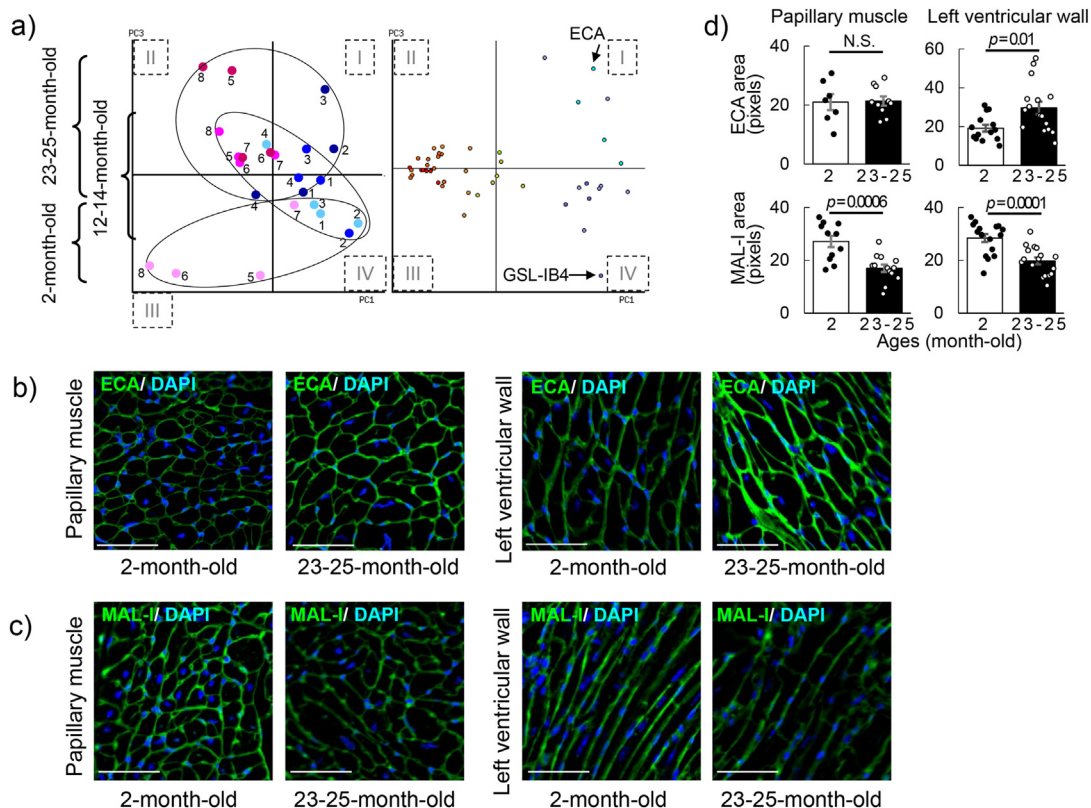


Fig. 5. Glycan changes in aging. (a) Eight regions of three mice per group in the different age groups (2, 12–14, and 23–25 months) were analyzed. PC3 represents aging. Closed circle (blue or pink) represents No. 1–4 or 5–8, respectively. Color gradients (light to dark) of dots reflect progressive senescence (i.e., young to aged). Left panel in the bi-plot: cardiac areas; right panel in the bi-plot: lectin replications. (b) The short-axes of cardiac tissues of 2-month-old and 23–25-month-old female mice were stained with *Erythrina cristagalli* agglutinin (ECA) (green) and 4',6-diamidino-2-phenylindole (DAPI) (blue) in the papillary muscle and the left ventricular wall regions on a set of the left and right sides ($n = 3$ per group). Scale bars are 50 μm . (c) The short-axes of cardiac tissues of 2-month-old and 23–25-month-old female mice were stained with *Maackia amurensis* lectin I (MAL-I) (green) and DAPI (blue) in the papillary muscle and the left ventricular wall regions on a set of the left and right sides ($n = 3$ per group). Scale bars are 50 μm . (d) Signal intensities binding ECA and MAL-I (upper and lower, respectively) were analyzed in 2-month-old and 23–25-month-old groups (open and closed bars, respectively). Left panel: papillary muscle; right panel: left ventricular wall ($n = 7$ –17 locations; 3 mice per group). $P < 0.05$. N.S. = no significant difference.

muscle at 23–25 months of age (6.0%) was lower than that at 2 months of age (8.4%), although the differences were not statistically significant (Fig. 6a). On the contrary, the stained area in the left ventricular wall (more epicardial side) decreased among the ages 2, 6, 12–14, and 23–25 months by 7.4%, 8.0%, 5.6%, and 5.6%, respectively, although the changes were not statistically significant (Fig. 6b). These results suggest that the amount of α -galactose residues in the microvessels, indicated by GSL-IB4, decrease at a rate depending on the location of the heart.

4. Discussion

Senescent cells are involved in various cardiovascular diseases [35,36]; therefore, identifying the molecular changes in the normal heart during aging will be useful for diagnosing and treating cardiac dysfunction. The cardiac extracellular matrices (ECM) are also involved in various cardiac diseases, both structural and non-structural related [37]. Glycans on ECM and glycolipids are important, not only for structural maintenance, but also for functions such as signal transduction. Changes in cell morphology related to changes in cell membranes and intercellular adhesion, as seen in Fig. 2b, reflect changes in the expression and localization of molecules on the plasma membrane (e.g., proteins, lipids, and their conjugated glycans). Therefore, age-related changes in glycans may represent one aspect of changes in cell morphology. The analysis of glycans, with various roles, has important implications for understanding these tissues.

Understanding the spatiotemporal changes in glycans and their role in tissue alteration is important in some organs during

aging or disease. For instance, glycans, such as disialyl-T antigen, are present at high levels, decreasing the core fucose levels in the tissues and sera of rats with cardiac hypertrophy [38]. In the hippocampus, the levels of gangliosides, including α 2-3 and 2–6 sialylated glycolipids, also decrease in the synaptic membrane during aging [39]. These glycans can be used as “medical indicators”. A previous report indicated that the amount of sialic acid on membrane proteins of human skin fibroblasts decreases with both cellular senescence and human aging, accompanied by suppressed the activation of skin fibroblasts [23,40,41]. Moreover, mesenchymal stem cells differentiated with a reduction in the amount of α 2-6linked sialic acid residues *in vitro* [42]. These changes in sialic acid residues were related to aging and function. In this study, it was suggested that the amount of sialic acid residues on the papillary muscle, which has an important role in mitral regulation, slightly decreases with cardiac hypertrophy during aging. On the contrary, it was reported that the levels of sialic acid residues of cardiomyocytes from 6-month-old female rats were higher than those of neonatal rats [43]. Considering that these reports focused on different age groups, our results suggest that the amount of sialic acid in cardiac tissue is from normal changes during aging in mice, and it is predicted that sialic acid in cardiac cells also has a functional role in the heart. However, fibrosis in mouse cardiac tissue, detected via WGA staining, increases with aging or myocardial infarction [44,45]. Further, WGA binds to sialic acid residues and chitin oligomers [34]; therefore, additional investigation is required to understand why these substances recognize different polarities, and caution should be taken when interpreting such data.

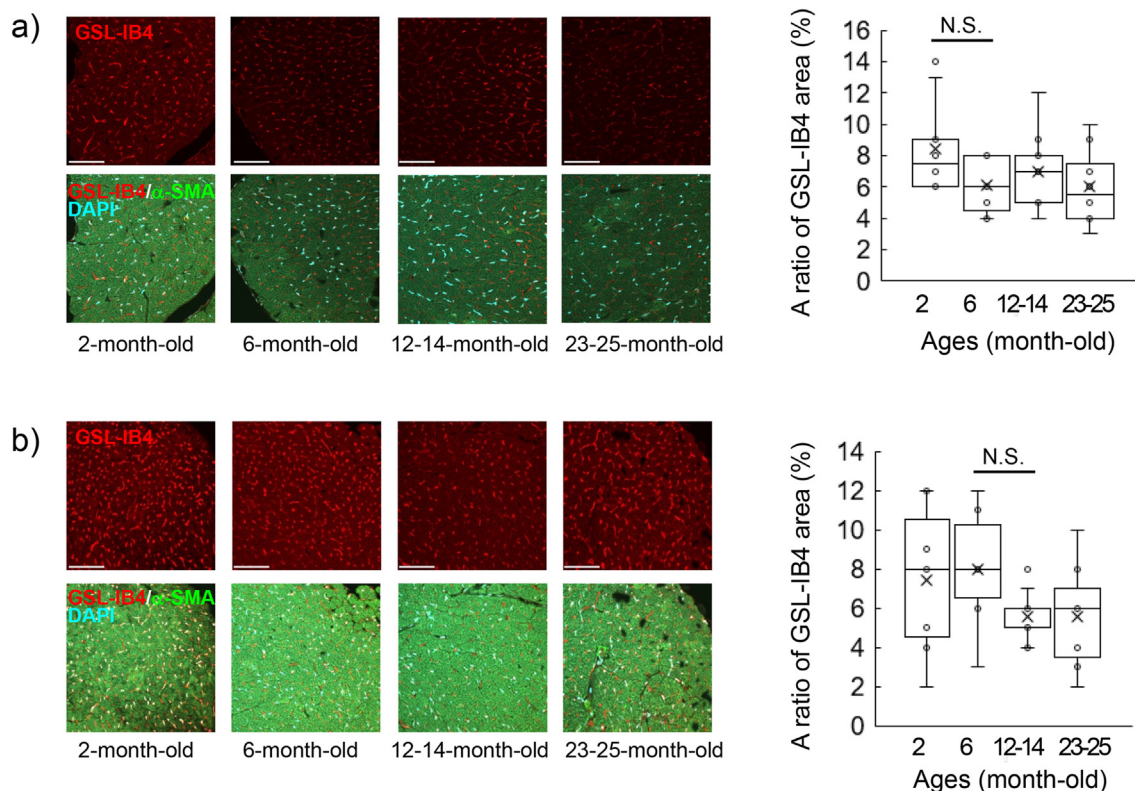


Fig. 6. Decrease in the number of cardiac microvessels with aging (a) Papillary muscles were stained for *Griffonia simplicifolia* lectin I (GSL-I) B4 (red) and combined with anti-alpha smooth muscle actin (SMA) antibody (green) and 4',6-diamidino-2-phenylindole (DAPI) (blue) signals in samples from mice aged 2, 6, 12–14, and 23–25 months (upper and lower, respectively) (60× magnification). Analysis was performed in the area without α -SMA staining. The values of the GSL-IB4-positive area of three female mice with seven to ten spots in every age group are shown in the box plot. (b) The left ventricular walls were stained for GSL-IB4 (red) and combined with anti- α -SMA antibody (green) and DAPI (blue) signals in samples from mice aged 2, 6, 12–14, and 23–25 months (upper and lower, respectively). The ratios of the GSL-IB4-positive area to the total area of three female mice with six to nine spots in every age group are shown in the box plot. Analysis was performed in the area without α -SMA staining. $P < 0.05$. N.S. = no significant difference. Scale bars are 50 μ m.

The present study also showed that the glycan profiles analyzed at each region were similar across all age groups. However, the reduction in the quantity of α -galactose residues in the microvessels, indicated by GSL-IB4, in the papillary muscle occurred at an earlier stage than that in the lateral side of the left ventricular wall (Fig. 6). These alterations matched well with the changes in glycan profiles in the lectin microarray data (Figs. 2b and 5a). The changes in the relative proportion (represented by number, endothelial thickness, surface area, and lumen diameter) of the microvessels on the cross-sectional area were not statistically significant; these may have been due to normal aging. Microvessel reduction would inhibit the supply of oxygen to cells and initiate cellular necrosis or undernutrition, causing the reduction of vascularity in various diseases. The difference in the rate of microvessel reduction between the medial and lateral sides of the left ventricle is thought to facilitate most heart failure cases in the elderly, which involves diastolic heart failure at different ages. Therefore, age-related glycan changes do not only cause structural changes in cardiac tissue but are also a signal of disease transitions. It should be noted that the detection of the α -galactose residue, which is the ligand of GSL-IB4, is limited in specific non-primates, such as mice. However, the reduction in the level of the glyco-epitope in mice has the potential to help elucidate the alteration in the number of human microvessels.

Mouse vascular endothelial cells can transform into smooth muscle cells or myofibroblasts via endothelial-to-mesenchymal transition (EMT) [46]. This reduction of α -galactose residues indicates that endothelial cells may undergo EMT and produce ECM, leading to increased fibrosis with age. Previously, we found that sialylated proteins were more abundant on the cell surface of cardiomyocytes and vascular endothelial cells than on fibroblasts, whereas asialo-glycoproteins were more abundant in fibroblasts [47]. The glycan profiles of human cardiac cells showed only a small change in cellular senescence without a significant difference. Although the glycan of cardiac constituent cells changed insignificantly at the cellular level, the reduction in sialic acid and α -galactose residues or the increase in asialo-glycan residues in aged mice seemed to occur changes in cell composition, such as a reduction in cardiomyocytes and vascular endothelial cells or an increase in fibroblasts. Further, although changes in the level of sialic acid observed during development differ with age, those of glycan on the cell surface regulate cell-ECM interactions and are accompanied by signaling [43]. Considering that changes in glycan content and localization in the mouse cardiac tissue were different in each region, the influence on each cell during aging may differ in individual cardiac regions with various cells *in vivo*.

The focus of lectin microarrays is only on glycoproteins, owing to the specificity of lectin and protein labeling methods. To understand the molecular changes in detail, it is necessary to identify glycans and glycopeptides. In addition, it is also necessary to have a good understanding of the specificity of lectins that recognize complex structures in the analysis of glycans using lectins. In a single-cell and nucleus transcriptomic analysis carried out recently, each cell-specific change was shown to occur in multiple cell types and organs, along with age-related changes [48,49]. Similar to a single-cell and nucleus transcriptomics research, a glycan atlas can be combined with various cellular analyses. Future studies should investigate details of glycan structural changes and identify the correlation between molecular changes at each region and functional alterations or disease onset.

The present study reports changes in glycan profiles depending on cardiac localization. We found that the rate of glycan profile changes differed based on cardiac localization and that the amount of sialic acid residues and α -galactose residues decreased in the papillary muscle and left ventricular wall. As the detection of α -

galactose residues showed a reduction in microvessels, the structure or the amount of glycans can indicate cardiac tissue conditions. Clinically, the validation of spatiotemporal changes during aging is important for successful patient management.

5. Conclusions

We analyzed glycan profiles for mice hearts and reported the unexpected finding that glycan profiles differ in each region of the cardiac tissue and change with aging. Obtaining and analyzing more detailed glycan information will be useful for the development of therapies involving the use of tissue regeneration, and for the elucidation of tissue functions and disease pathogenesis mechanisms.

Funding

This work was supported by the Ministry of Education, Culture, Sports, Science and Technology of Japan [grant numbers 16K19098 and 21K11666 to Y.I. and 21K19754 to M.T.] and the National Center for Child Health and Development [grant number 29–1 to M.T.].

Author contributions

YI designed the overall study, performed the experiments, analyzed the data, and prepared the manuscript. YK prepared the mouse cardiac tissue, and YH prepared the thin sections and performed HE staining. YM, KS, and TI contributed to data analysis. CNO and AK provided the techniques for laser micro dissection and lectin microarray analysis. NS, MU, YT, and TK provided suggestions. MT designed the study and edited the manuscript. All authors have read and approved the final manuscript

Data availability

The data underlying this article are available in the article, online supplementary materials, and in a database at LM-GlycomeAtlas at https://glycosmos.org/lm_glycomeatlas/index. This manuscript has been posted on preprint servers but not yet published. <https://doi.org/10.21203/rs.3.rs-960240/v1>.

Ethics approval

The animal protocol was approved by the Animal Ethics and Experimentation Committee of Tokyo Metropolitan Institute of Gerontology (TMIG) (No. 17020 and 20010), and all methods were performed at TMIG in accordance with the relevant guidelines and regulations. This study is reported in accordance with ARRIVE guidelines (<https://arriveguidelines.org>).

Declaration of competing interest

The authors declare no competing or financial interests.

Acknowledgments

We would like to thank Atsuko Seki for her critical suggestions, Maki Yoshida for her technical advice, Editage (www.editage.com) for English language editing, and Science Graphics. Co., Ltd. for help with preparing the graphical abstract.

Appendix A. Supplementary data

Supplementary data to this article can be found online at <https://doi.org/10.1016/j.reth.2022.12.009>.

References

- [1] Triposkiadis F, Xanthopoulos A, Butler J. Cardiovascular aging and heart failure: JACC review topic of the week. *J Am Coll Cardiol* 2019;74:804–13.
- [2] Fish KM, Mieczko J, Hajjar RJ. Of mice and men. *Circ Res* 2018;123:1109–11.
- [3] Niccoli T, Partridge L. Ageing as a risk factor for disease. *Curr Biol* 2012;22:R741–52.
- [4] North BJ, Sinclair DA. The intersection between aging and cardiovascular disease. *Circ Res* 2012;110:1097–108.
- [5] Thiene G, Valente M. Degenerative, non-atherosclerotic cardiovascular disease in the elderly: a clinico-pathological survey. *Aging (Milano)* 1990;2:231–44.
- [6] French JK, Hellkamp AS, Armstrong PW, Cohen E, Kleiman NS, O'connor CM, et al. Mechanical complications after percutaneous coronary intervention in ST-elevation myocardial infarction (from APEX-AMI). *Am J Cardiol* 2010;105:59–63.
- [7] Qian G, Liu HB, Wang JW, Wu C, Chen YD. Risk of cardiac rupture after acute myocardial infarction is related to a risk of hemorrhage. *J Zhejiang Univ - Sci B* 2013;14:736–42.
- [8] Walts PA, Gillinov AM. Survival after simultaneous left ventricular free wall, papillary muscle, and ventricular septal rupture. *Ann Thorac Surg* 2004;78:e77–8.
- [9] Bader F, Manla Y, Atallah B, Starling RC. Heart failure and COVID-19. *Heart Fail Rev* 2021;26:1–10.
- [10] Lian J, Jin X, Hao S, Cai H, Zhang S, Zheng L, et al. Analysis of epidemiological and clinical features in older patients with coronavirus disease 2019 (COVID-19) outside wuhan. *Clin Infect Dis* 2020;71:740–7.
- [11] Long B, Brady WJ, Koyfman A, Gottlieb M. Cardiovascular complications in COVID-19. *Am J Emerg Med* 2020;38:1504–7.
- [12] Lan J, Ge J, Yu J, Shan S, Zhou H, Fan S, et al. Structure of the SARS-CoV-2 spike receptor-binding domain bound to the ACE2 receptor. *Nature* 2020;581:215–20.
- [13] Shang J, Ye G, Shi K, Wan Y, Luo C, Aihara H, et al. Structural basis of receptor recognition by SARS-CoV-2. *Nature* 2020;581:221–4.
- [14] Wang Q, Zhang Y, Wu L, Niu S, Song C, Zhang Z, et al. Structural and functional basis of SARS-CoV-2 Entry by using human ACE2. *Cell* 2020;181:894–904 e899.
- [15] Wrapp D, Wang N, Corbett KS, Goldsmith JA, Hsieh CL, Abiona O, et al. Cryo-EM structure of the 2019-nCoV spike in the prefusion conformation. *Science* 2020;367:1260–3.
- [16] Yan R, Zhang Y, Li Y, Xia L, Guo Y, Zhou Q. Structural basis for the recognition of SARS-CoV-2 by full-length human ACE2. *Science* 2020;367:1444–8.
- [17] Litvinukova M, Talavera-Lopez C, Maatz H, Reichart D, Worth CL, Lindberg EL, et al. Cells of the adult human heart. *Nature* 2020;588:466–72.
- [18] Elder SS, Emmerson E. Senescent cells and macrophages: key players for regeneration? *Open Biol* 2020;10:200309.
- [19] He S, Sharpless NE. Senescence in Health and disease. *Cell* 2017;169:1000–11.
- [20] Song P, An J, Zou MH. Immune clearance of senescent cells to combat ageing and chronic diseases. *Cells* 2020;9.
- [21] Childs BG, Li H, Van Deursen JM. Senescent cells: a therapeutic target for cardiovascular disease. *J Clin Invest* 2018;128:1217–28.
- [22] Endo T. Glycobiology of alpha-dystroglycan and muscular dystrophy. *J Biochem* 2015;157:1–12.
- [23] Itakura Y, Sasaki N, Kami D, Gojo S, Umezawa A, Toyoda M. N- and O-glycan cell surface protein modifications associated with cellular senescence and human aging. *Cell Biosci* 2016;6:14.
- [24] Miura Y, Hashii N, Ohta Y, Itakura Y, Tsumoto H, Suzuki J, et al. Characteristic glycopeptides associated with extreme human longevity identified through plasma glycoproteomics. *Biochim Biophys Acta Gen Subj* 2018;1862:1462–71.
- [25] Itakura Y, Kuno A, Toyoda M, Umezawa A, Hirabayashi J. Podocalyxin-targeting comparative glycan profiling reveals difference between human embryonic stem cells and embryonal carcinoma cells, S5. *Glycomics & Lipidomics*; 2013. p. 4.
- [26] Kuno A, Itakura Y, Toyoda M, Takahashi Y, Yamada M, Umezawa A, et al. Development of a data-mining System for differential profiling of cell glycoproteins based on lectin microarray. *J Proteomics Bioinf* 2008;1:68–72.
- [27] Pilobello KT, Slawek DE, Mahal LK. A ratiometric lectin microarray approach to analysis of the dynamic mammalian glycome. *Proc Natl Acad Sci U S A* 2007;104:11534–9.
- [28] Matsuda A, Kuno A, Ishida H, Kawamoto T, Shoda J, Hirabayashi J. Development of an all-in-one technology for glycan profiling targeting formalin-embedded tissue sections. *Biochem Biophys Res Commun* 2008;370:259–63.
- [29] Matsuda A, Higashi M, Nakagawa T, Yokoyama S, Kuno A, Yonezawa S, et al. Assessment of tumor characteristics based on glycoform analysis of membrane-tethered MUC1. *Lab Invest* 2017;97:1103–13.
- [30] Zou X, Yoshida M, Nagai-Okatani C, Iwaki J, Matsuda A, Tan B, et al. A standardized method for lectin microarray-based tissue glycome mapping. *Sci Rep* 2017;7:43560.
- [31] Nagai-Okatani C, Aoki-Kinoshita KF, Kakuda S, Nagai M, Hagiwara K, Kiyohara K, et al. A novel Visualization tool for lectin microarray-based glycomic profiles of mouse tissue sections. *Molecules* 2019;24.
- [32] Tateno H, Kuno A, Itakura Y, Hirabayashi J. A versatile technology for cellular glycomics using lectin microarray. *Methods Enzymol* 2010;478:181–95.
- [33] Ding P, Huang J, Battiprolu PK, Hill JA, Kamm KE, Stull JT. Cardiac myosin light chain kinase is necessary for myosin regulatory light chain phosphorylation and cardiac performance in vivo. *J Biol Chem* 2010;285:40819–29.
- [34] Itakura Y, Nakamura-Tsuruta S, Kominami J, Tateno H, Hirabayashi J. Sugar-binding profiles of chitin-binding lectins from the hevein family: a comprehensive study. *Int J Mol Sci* 2017;18.
- [35] Childs BG, Durik M, Baker DJ, Van Deursen JM. Cellular senescence in aging and age-related disease: from mechanisms to therapy. *Nat Med* 2015;21:1424–35.
- [36] Sheydina A, Riordon DR, Boheler KR. Molecular mechanisms of cardiomyocyte aging. *Clin Sci (Lond)* 2011;121:315–29.
- [37] Rienks M, Papageorgiou AP, Frangogiannis NG, Heymans S. Myocardial extracellular matrix: an ever-changing and diverse entity. *Circ Res* 2014;114:872–88.
- [38] Nagai-Okatani C, Minamino N. Aberrant glycosylation in the left ventricle and plasma of rats with cardiac hypertrophy and heart failure. *PLoS One* 2016;11:e0150210.
- [39] Sato Y, Akimoto Y, Kawakami H, Hirano H, Endo T. Location of sialoglycoconjugates containing the Sia(alpha)2-3Gal and Sia(alpha)2-6Gal groups in the rat hippocampus and the effect of aging on their expression. *J Histochem Cytochem* 2001;49:1311–9.
- [40] Itakura Y, Sasaki N, Toyoda M. Qualitative and quantitative alterations in intracellular and membrane glycoproteins maintain the balance between cellular senescence and human aging. *Aging (Albany NY)* 2018;10:2190–208.
- [41] Sasaki N, Itakura Y, Toyoda M. Sialylation regulates myofibroblast differentiation of human skin fibroblasts. *Stem Cell Res Ther* 2017;8:81.
- [42] Tateno H, Saito S, Hiemori K, Kiyoi K, Hasehira K, Toyoda M, et al. alpha 2-6 sialylation is a marker of the differentiation potential of human mesenchymal stem cells. *Glycobiology* 2016;26:1328–37.
- [43] Contessotto P, Ellis BW, Jin C, Karlsson NG, Zorlutuna P, Kilcoyne M, et al. Distinct glycosylation in membrane proteins within neonatal versus adult myocardial tissue. *Matrix Biol* 2020;85–86:173–88.
- [44] Emde B, Heinen A, Godecke A, Bottermann K. Wheat germ agglutinin staining as a suitable method for detection and quantification of fibrosis in cardiac tissue after myocardial infarction. *Eur J Histochem* 2014;58:2448.
- [45] Pandya K, Kim HS, Smithies O. Fibrosis, not cell size, delineates beta-myosin heavy chain reexpression during cardiac hypertrophy and normal aging in vivo. *Proc Natl Acad Sci U S A* 2006;103:16864–9.
- [46] Kovacic JC, Dimmeler S, Harvey RP, Finkel T, Aikawa E, Krenning G, et al. Endothelial to mesenchymal transition in cardiovascular disease: JACC state-of-the-Art review. *J Am Coll Cardiol* 2019;73:190–209.
- [47] Itakura Y, Sasaki N, Toyoda M. Glycan characteristics of human heart constituent cells maintaining organ function: relatively stable glycan profiles in cellular senescence. *Biogerontology* 2021;22:623–37.
- [48] Tabula Muris Consortium. A single-cell transcriptomic atlas characterizes ageing tissues in the mouse. *Nature* 2020;583:590–5.
- [49] Vidal R, Wagner JUG, Braeuning C, Fischer C, Patrick R, Tombar L, et al. Transcriptional heterogeneity of fibroblasts is a hallmark of the aging heart. *JCI Insight* 2019;4.